Journal of
Composites Science

MDPI

Review

Fracture Mechanisms and Toughness in Polymer Nanocomposites: A Brief Review

Theodor Stern [1] and Gad Marom [2,*]

[1] Department of Chemical Engineering, Biotechnology and Materials, Faculty of Engineering, Ariel University, Ariel 40700, Israel; theodorst@ariel.ac.il
[2] Casali Center of Applied Chemistry, The Institute of Chemistry and the Center for Nanoscience and Nanotechnology, The Hebrew University of Jerusalem, Jerusalem 91904, Israel
* Correspondence: gad.marom@mail.huji.ac.il

Abstract: This article underlines the observation that, unlike the underperformance of nanocomposites in as far as their static mechanical properties of modulus and strength are concerned, fracture toughness exhibits exceptional behavior. This is attributed to the fact that fracture toughness expresses a measure of the energy absorbed in crack propagation, namely, the energy involved in creating new surface area, which, in turn, is controlled by a specific type of energy-dissipating interaction of the crack front with nanoparticles. This concise review focuses on two micromechanisms that are considered representative of energy dissipation due to their frequent presence in nanocomposites of both nanoparticles and nanofibers. Examples taken from recent relevant articles are presented to showcase fracture toughness improvements by nanoparticles.

Keywords: polymer nanocomposites; fracture mechanisms; fracture toughness

1. Introduction

The invention of carbon nanotubes, with their anticipated extremely high mechanical properties, has generated significant interest in the prospects of utilizing them for ultra-high-mechanical-property composite materials. Moreover, this discovery has instigated a broader interest in a new class of composites, namely, nanocomposites, wherein polymer matrices are reinforced by various newly invented nanofillers. Obviously, classical micromechanical models and mechanisms have been implicit a priori to explain the behavior of nanocomposites, with the expectation that small concentrations of nanoreinforcement can lead to extremely high mechanical properties.

However, as shown in a *Composites Encyclopedia* chapter [1], in most of the examples, the empirical values of mechanical properties of different nanocomposites fall significantly below the expected ones. Concomitantly, the application of classical micromechanical models and mechanisms fail, by and large, to predict the mechanical properties of nanocomposites. Indeed, a number of examples exist in the literature, where it is observed that low contents that are well dispersed exhibit an apparent linear behavior in the strength and modulus; yet, the actual mechanical properties are much below the expectations. This can be explained by the fact that there are too many unknowns regarding nanofillers, which would be accountable for the large difference between the predicted and the measured properties, e.g., the inherent mechanical properties (the modulus and the strength) of the nanoparticles. Are they 2D or 3D aligned or randomly dispersed in the matrix? Are they fully exfoliated? What is their actual aspect ratio? It is also unclear whether or not the classical stress transfer mechanism is relevant to nanocomposites.

Unlike the underperformance of nanocomposites in as far as their static mechanical properties of modulus and strength are concerned, fracture toughness exhibits exceptional behavior. This is attributed to the fact that fracture toughness expresses a measure of the energy absorbed in crack propagation, namely, the energy involved in creating new surface

check for updates

Citation: Stern, T.; Marom, G. Fracture Mechanisms and Toughness in Polymer Nanocomposites: A Brief Review. *J. Compos. Sci.* **2024**, *8*, 395. https://doi.org/10.3390/jcs8100395

Academic Editor: Chi-Hui Tsou

Received: 8 August 2024
Revised: 23 September 2024
Accepted: 25 September 2024
Published: 1 October 2024

Copyright: © 2024 by the authors. Licensee MDPI, Basel, Switzerland. This article is an open access article distributed under the terms and conditions of the Creative Commons Attribution (CC BY) license (https://creativecommons.org/licenses/by/4.0/).

area, which, in turn, is controlled by the specific type of energy-dissipating interaction of the crack front with nanoparticles [1]. Consequently, nanofillers are used in relatively small quantities to toughen pristine polymer matrices and fiber-reinforced composites.

The question of whether nanoparticles affect fracture toughness (and other physical properties, e.g., the glass transition) was recently addressed in two opinion articles presenting a perspective on the structure and properties of nanocomposites [2,3]. The conclusion of these articles highlights the idea that the nanometric or molecular structure of nanocomposites is influenced by several factors: the type and extent of exfoliation of nanoparticles, their dispersion, and their interaction with the polymer matrix. Specifically, the articles distinguish between two types of structures: solid solutions and molecular composites. In cases where there are weak or no interactions between the nanoparticles and the matrix, the result is a solid solution. Conversely, when strong interfacial bonding occurs, creating a network of continuous molecular chains, the structure is classified as a molecular composite. Such structural features—joined with specific characteristics of the nanoparticles (as listed hereafter)—are expected to control the toughness of nanocomposites.

The aim of this brief review is to present different cases of the toughening of nanocomposites and to analyze the contribution of nanofillers to the enhancement of energy dissipation during fracture propagation. An emphasis is made on two specific mechanisms of nanofiller–crack front interactions that trigger secondary microprocesses in which the absorption of energy translates to a higher fracture surface energy. The energy that is invested in such microprocesses depends mostly on the geometric aspect ratio of the nanofillers (nanoparticles, nanoplatelets, and nanofibers), area-to-volume ratio of the nanofillers, their type, and the interfacial interactions with the matrix. In the review below, we focus on two micromechanisms that are considered representative of energy dissipation due to their frequent presence in nanocomposites. They refer to nanoparticles and nanofibers.

2. Fracture Mechanics and Toughness of Polymer Nanocomposites

Fracture toughness is regarded as a significant property in determining whether the material is suitable for certain specific applications without failing. To study the effects of nanofillers on the fracture toughness of polymer nanocomposites, a distinction should be made based on the typology of the nanofillers, e.g., CNTs; plate-like nanofillers, either graphene or clay; and nanoparticles. A literature survey of studies on the fracture toughness of nanocomposites shows that this property is enhanced significantly for even minor additions of different nanoparticles, demonstrating that various mechanisms are active in the energy absorption process [1].

In contrast to the static properties of strength and stiffness, the fracture mechanics and toughness of nanocomposites are not influenced by an effective stress transfer mechanism. Instead, they depend on the geometry of the nanoparticles. The key factor affecting toughness is the interaction between the crack front and the nanoparticles, which can interrupt or stop crack propagation. Those interactions are so highly energetic that they essentially dominate the fracture process. They can be orders of magnitude more powerful than the intrinsic fracture processes involved in breaking the matrix, whose contribution to the overall fracture energy is relatively negligible and can in fact be disregarded.

In general, we identify two prototypical interactions, depending on the geometry of the nanoparticles as expressed by their aspect ratio. In the first mechanism, which applies to tube or rode-like geometries, fracture energy is dissipated initially in the shear failure of the particle/matrix interface followed by the work of friction pulling out the nanoparticles from the matrix. The second mechanism, which applies to low aspect ratio particles, for example, nanospheres, incurs particle–crack front interactions, wherein the particles act as pinning positions that slow down the crack front propagation. This classification, which divides nanocomposites into two groups based on the aspect ratio of their nanoreinforcements, is somewhat simplistic. While it addresses the primary mechanisms of fracture surface energy absorption, it is clear that other mechanisms—whether acting independently or

in combination, including those within the matrix—can also contribute to the overall energy absorption.

2.1. Nanofiber Pull-Out

Having no restrictions on the actual dimensions and aspect ratio of the reinforcement, the classical model (Equation (1)) that describes the pull-out energy dissipated in fracture of discontinuous fiber reinforced composites should apply for nanoreinforcements as well. Moreover, a number of reports exist, which show that strongly bonded, surface-treated CNT can bridge the crack front and then eventually break crack propagation while dissipating high fracture energy by both breaking and pull-out. A pull-out process is depicted in Figure 1, showing a section of a nanorod of length l—from its end to the main fracture plane—as it is being pulled-out due to external stress. Considering the fiber pull-out frictional energy, it is given by

$$\gamma_{po} = \frac{\phi_f \tau_{if} l^2}{24r} \quad (1)$$

where γ_{po} is the pull-out component of the fracture surface energy, ϕ_f is the volume content of the nanorods, τ_{if} is the fiber/matrix interfacial shear strength, and l and r are the fiber length and radius, respectively [1]. Equation (1) expresses the frictional energy dissipated in retrieving a rod-like nanoparticle from the matrix at the crack tip. This mechanism interferes with crack propagation to the extent that it controls the fracture process in the nanocomposite and dominates its total fracture surface energy.

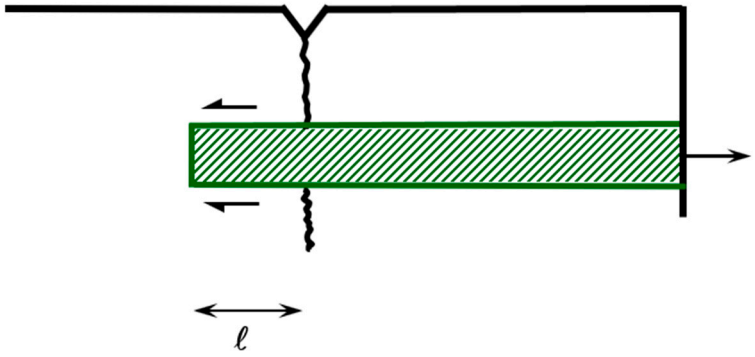

Figure 1. Illustrations of the pull-out mechanism in nanocomposites reinforced with high aspect ratio nanoparticles, like carbon nanotubes, depicting a segment of a nanorod of length l from its end to the main fracture plane. This segment is shown being extracted from the matrix by external stress. The fracture surface energy is contributed by the frictional work dissipated at the nanofiber/matrix interface. The black arrows mark the pull-out and the frictional stresses, respectively, operating on the nanorod (in green).

A recent example of a huge contribution (85–145%) of surface-treated CNT to the Mode II interlaminar fracture toughness (ILFT) of interleaved epoxy/carbon fabric laminates demonstrates clearly both the protruding CNTs and the increased surface roughness [4].

2.2. Crack Front Bowing

A classical model of the crack arrest mechanism known as crack front bowing was proposed by Lange [5] for low aspect ratio particles and is presented schematically in Figure 2. According to this model, as the crack front, which is temporarily held up by nanoparticle inhomogeneities, bows outward, the fracture energy should increase due to the elongation of the crack path. The model quantifies this increase in fracture energy based on the additional length of the bowed crack front, which depends on the distance between particles and their size and volume fraction. This significant energy absorption is evident from the pronounced roughness of the fracture surface, which can be quantitatively evaluated using a microscopic evaluation of the bow's marks on the fracture surface [5].

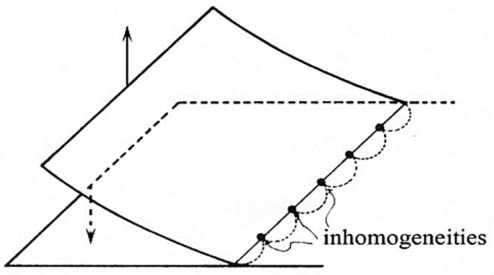

Figure 2. Schematics of a moving crack front pinned momentarily by a row of nanoparticles within the matrix, which are identified as inhomogeneities. The bow span increases by gradually bowing out under the action of the applied fracture stress, until its eventual catastrophic breaking away, which is to be stopped by the next row of nanoparticles. The surplus fracture surface energy is accounted for by a continuous series of crack arrest–breakaway catastrophic crack jump events, contributing to an overall controlled fracture propagation process (after Lange [5]). Arched dotted lines indicate the crack bowing and pinning trajectories; the arrows indicate the applied Mode I opening load directions.

The crack front bowing mechanisms comprises three stages: (i) arresting the advancing crack front by its pinning at an array of nanoparticles; (ii) bowing out of the crack front, leaving its bow-like marks on the nascent fracture surface; and (iii) propagating by a catastrophic breaking away of the crack front from the pinning points all the way to the next array of nanoparticles. The surplus energy is accounted for by a continuous series of crack arrest–breakaway events, where the overall fracture propagation process is controlled by energy loss in a series of catastrophic crack jump steps.

3. Examples of Fracture in Nanocomposites

Fracture toughness is regarded a significant property in determining whether the material is suitable for certain specific applications without fracturing [6,7]. This feature stands out in view of our recent claim regarding the mechanical properties of nanocomposites, suggesting that, whereas strength and stiffness do not perform up to the expectations, their fracture toughness is outstanding. As shown in [1], the toughness of nanocomposites is enhanced significantly for even minor additions of different nanoparticles, demonstrating that either or both mechanisms, and other ones, are active in the energy absorption process. Below, we showcase a number of examples taken from most recent relevant articles.

The examples of nanocomposites listed below may be divided according to two main classifications: 1- nanocomposites reinforced with nanotubes (examples: 5;8;12;14;15) and with nanofibers (examples: 2;3;7;21–24), corresponding mainly to the above-described fiber pull-out mechanism and 2- nanocomposites reinforced with nanoparticles (examples: 1;4;6;9–11;13;16–20), corresponding mainly to the above-described crack front bowing mechanism.

Examples include the following:

1. Nanocomposite films of pullulan reinforced by starch nanoplatelets (biomimicking a leaf vein network structure) exhibited enhanced mechanical properties: specifically, toughness values of pullulan with 1% *w*/*w* nanoplatelets reached up to 69.65 MJ m^{-3}, being 223% higher than that of the neat pullulan film [8].
2. Nanocomposites of an epoxy matrix, reinforced by a hybrid nanofiller consisting of exfoliated montmorillonite clay layers inside a fibrous network of cellulose nanofibers (CNF), were developed by using a sustainable green hybrid nanofiller. The inclusion of 0.5 phr of only CNF (1.085 MPa $m^{1/2}$) enhanced the fracture toughness value by 25% compared to neat epoxy (from 0.866 MPa $m^{½}$ to 1.085 MPa $m^{½}$). Although the addition of nanoclay alone did not exhibit a significant improvement, the addition of 0.5 phr of the hybrid nanofiller resulted in a drastic increase of 32.3% in the K_{IC} value (1.176 MPa $m^{1/2}$) [9].

3. Efficient balance between hardness/toughness and transparency was obtained in PMMA-based nanocomposites, by the simultaneous addition of controlled amounts of poly (vinyl butyral) (PVB) and titania (TiO_2) nanofibers.
   Accordingly, PMMA/PVB/TiO_2 composites containing 3 wt% and 5 wt% nanoparticles exhibited a significantly higher fracture toughness compared with the neat polymer: 2.73 (0.128) MPa $m^{1/2}$, 4.24 (0.154) MPa $m^{1/2}$, and 3.16 (0.495) MPa $m^{1/2}$, respectively. Also, the fracture toughness of the PMMA nanocomposite was increased by 55% by the addition of 3 wt% titania nanoparticles, while maintaining a high transmittance above 75–80% in the visible domain [10].
4. Thermo-conductive and healable nanocomposites, exhibiting a nacre-like hierarchical architecture, produced by incorporating boron nitride nanosheets (BNNSs) into a polyurethane matrix through a bottom-up assembly process and lamination technology, resulted in a simultaneous enhancement in stiffness of 5.3 times, in strength of 20.1 times, and in fracture toughness of 16.4 times in the nacre-mimetic nanocomposite compared to those of the polyurethane matrix [11].
5. Multiwall carbon nanotube (MWCNT)-MXene hybrid nanofillers-based epoxy nanocomposites exhibited a fracture toughness of 1.79 MPa·$m^{1/2}$ with the addition of 1 wt% MWCNT/MXene hybrid, as compared to only 0.97 MPa·$m^{1/2}$ of the neat epoxy measured, primarily attributed to crack deflection and filler debonding mechanisms [12].
6. A nacre-inspired lightweight and thermally conductive boron nitride nanosheet/epoxy layered (BNNEL) nanocomposite, exhibited a high fracture toughness of 4.22 MPa·$m^{1/2}$ at a boron nitride nanosheet loading of 2.08 vol.%, being seven-fold higher than the fracture toughness of the pure epoxy matrix [13].
7. Poly(arylene ether ketone)-based nanocomposites, containing 0.1% of cellulose nanofibers (CNF), preliminarily dispersed in the monomer prior to polymerization, increased both tensile strength and elongation and improved the tensile fracture toughness to approximately two-fold, to 44.1 MJ m^{-3}, as compared to 21.3 MJ m^{-3} in the pure matrix. An amount of 0.1% was found to be the maximum CNF amount, which did not reduce the molecular weight of the poly(arylene ether ketone) matrix. At 0.1 wt% CNF, both tensile strength and elongation increased about 30% and 83%, respectively, and the tensile toughness was increased by 207%, through the interaction between the matrix and the nanofiber filler [14].
8. A silicone rubber-based stretchable piezoresistive strain sensor nanocomposite was synergistically toughened, using multiwalled carbon nanotubes (MWCNTs) and molybdenum disulfide (MoS2). A toughness of 8.46 kJ/m^3 was obtained at 5 phr MWCNT-MoS2 hybrids, being 125% higher than the unfilled rubber, indicating a significant synergistic effect of the hybrid filler [15].
9. The effect of random Graphene Nanoplatelets (GNP) versus aligned Fe3O4-GNP nanoplatelets on the fracture resistance of epoxy nanocomposites was investigated, attempting at optimizing fracture properties like the crack growth resistance (KIC), critical stress in tensity factor (GIC), and critical crack tip opening displacement (CTODc). The results indicated a significant increase in fracture toughness of 27.39% and 58.64% for the respective aligned Fe3O4-GNP and GNP loadings, at 0.600 wt%, (1.2 MPa $m^{1/2}$ and 1.49 MPa $m^{1/2}$, respectively, as compared to 0.94 MPa $m^{1/2}$, for pure epoxy) [16].
10. Nanocomposites of PMMA-ZrO_2 were investigated for biomedical and denture implant applications. The fracture toughness consistently increased with increasing nanofiller content, reaching a maximum value of 6.58 MPa $m^{½}$, obtained at a 5% nanofiller content (as compared to about 5 MPa $m^{½}$ for the neat PMMA), and drastically decreased with higher nanofiller contents [17].
11. A "bottom-up" manufacturing method of montmorillonite-based nanocomposite material was investigated with the purpose of mimicking the freshwater mussel Cristaria plicata's nacre architecture and properties by the self-assembly of montmo-

rillonite/chitosan/polyvinyl alcohol and low-temperature lamination process—thus resembling the mussel's shell consisting of a combination of aragonite and organic matter arranged in an oriented "Brick-and-Mortar" pattern. A fracture toughness of ~2.2 MPa $m^{1/2}$ was obtained for the artificial nacre, which is only slightly lower than that of natural C. plicata nacre (~2.4 MPa $m^{1/2}$) [18].

12. Epoxy-based nanocomposites reinforced by carbon nanotubes (CNT) sponge were prepared in order to solve the difficulties associated with the dispersion and re-agglomeration of the CNTs. The K_{IC} value of the nanocomposites reached 1.86 MPa $m^{1/2}$, being 104% higher compared with that of the matrix ($K_{IC(Epoxy)}$ = 0.91 MPa $m^{1/2}$). The improved fracture properties of nanocomposites were mainly attributed to crack deflection and bifurcation [19].
13. The effect of nanofillers dimensions on the mechanical and toughness properties of epoxy resin was investigated using two-dimensional boron nitride (BN) and zero-dimensional silica (SiO_2). At 3.0 wt%, K_{IC} values of 1.020 MPa $m^{0.5}$ and 1.135 MPa $m^{0.5}$, were obtained for epoxy/BN and epoxy/SiO_2, respectively, as compared to 0.597 MPa $m^{0.5}$ for the neat epoxy [20].
14. Nanocomposites consisting of epoxy/carbon fabric (CF) laminate composites with inclusions of 0.5 to 2 wt% multiwalled carbon nanotubes (MWCNT) were analyzed. The volume fraction of carbon fabric was 0.65 for all the laminates. The tensile and fracture properties of the composites improved significantly with MWCNT content, but declined beyond 1 wt%, due to agglomeration. The fracture toughness properties of epoxy nano and multiscale composites were 3.0 MPa $m^{1/2}$ and 19.1 MPa $m^{1/2}$, respectively, as compared to 1.8 MPa $m^{1/2}$ for the neat epoxy [21].
15. Carboxyl-functionalized multiwalled carbon nanotubes (COOH-MWCNTs) and a thermoplastic polyetherimide (TP), were combined with each of the two types of epoxy resins, namely, diglycidyl ether of bisphenol A (DGEBA) and tetraglycidyl-4,4′-diaminodiphenylmethane (TGDDM). The Mode-I fracture toughness (G_{IC}), of the epoxy blends exhibited a synergistic enhancement in the fracture toughness of the resin. The highest obtained values for DGEBA were with 0.3% CNT and 10% TP: 182.6 J m^{-2}, as compared to 96 J m^{-2} for the pure matrix, and for TGDDM with 0.3% CNT and 10% TP: 130.7 J m^{-2}, as compared to 61.3 J m^{-2} for the pure matrix [22].
16. Epoxy nanocomposites, with two-dimensional (2H polytype) molybdenum disulfide (MoS_2) nanoplatelets as a filler, functionalized by simultaneous in situ exfoliation in the presence of cetyltrimethylammonium bromide (CTAB), were fabricated via sonication, ranging in content from 0.1 wt% up to 1 wt%.
    The maximum fracture properties were obtained with an f-MoS_2 nanoplatelets loading of 0.25 wt% as it shows K_{IC} value of 1.52 MPa $m^{1/2}$, corresponding to an improvement of 81% when compared to neat epoxy (0.84 MPa $m^{1/2}$), which declined for higher nanoplatelet loads [23].
17. Carbon black-filled epoxy nanocomposites were produced with 1%, 3%, 5%, and 10% filler loading. The fracture toughness value of all nanocomposites showed an increasing trend with the increase in the CNBFs loading up to 5%, beyond which a pronounced decline was observed—the highest fracture toughness obtained reached 2.3 MPa $m^{1/2}$, compared to 0.22 MPa $m^{1/2}$ for the pure epoxy matrix [24].
18. Epoxy nanocomposites with ozone and tetraethylenepentamine (TEPA)-functionalized nanodiamonds (ozone/TEPA ND) were produced to improve thermal conductivity and fracture resistance by enhancing interfacial interactions. The highest fracture toughness was achieved with 0.5 wt% ozone/TEPA ND composites (16.1 MPa $m^{1/2}$), which was 121% higher than with the pristine non-functionalized ND nanocomposite [25].
19. Poly(butylene terephthalate) (PBT) nanocomposites were reinforced with montmorillonite (MMT) and nano precipitated calcium carbonate (NPCC). The highest fracture toughness values were obtained at 6% nanofiller content for each of the two nanocomposite types, i.e., 2.01 MPa $m^{1/2}$ and 1.86 MPa $m^{1/2}$ for the PBT-MMT and PBT-NPCC

nanocomposites, respectively, being 57% and 45% higher than the fracture toughness of the neat matrix (1.28 MPa $m^{1/2}$), respectively [26].

20. A green and efficient method was used to prepare epoxy/GO nanocomposites by in situ polymerization for synthesizing nanocomposites, eliminating the need for organic solvents and surfactants. EP/GO nanocomposites with 0.6 wt% of GO exhibited a fracture toughness of 1.62 MJ m^{-3} compared to the fracture toughness of the pure epoxy of 0.66 MJ m^{-3} [27].
21. Hybrid ternary systems of thermoplastic/Cloisite clay/thermoset polyester, containing a thermoplastic additive (copolymer of methyl methacrylate and styrene, were prepared and analyzed. While a consistent decrease in the tensile stress was observed for all tested nanocomposites formulations, as compared to the pristine matrix—all tested samples exhibited significant fracture toughness enhancement. Depending on the nanocomposite formulation type, a maximum fracture toughness enhancement of 66% was obtained [28].
22. Epoxy nanocomposites were prepared with aramid nanofibers (ANFs), which were surface-functionalized with chlorinated cellulose nanocrystals and 3 -glycidoxypropyltrimethoxysilane, intended at improving compatibility with the epoxy matrix. At 1.5 wt% nanofiber content, the Young's modulus and tensile strength were increased by 15.1% and 10.1%, respectively, and the fracture toughness exhibited a 250% increase, as compared to the neat epoxy resin [29].
23. Nature-derived nanocellulose (NC) reinforcement was used to fabricate shape memory epoxy-based nanocomposites (SMEPNs). NC acetylation modification was performed to improve the compatibility between NCs and the epoxy matrix. SMEPNs with 0.06 wt% of the nanofibers resulted in a fracture toughness improvement of over 42%, along with the enhancement of only several % in the elastic modulus, and ultimate strength [30].
24. Epoxy nanocomposites with aramid nanofibers (ANFs) functionalized with glycidyl ether silane exhibited a Young's modulus and tensile strength increase of 16.8% and 14.0%, respectively, at 1 wt% ANFs, and a fracture toughness increase by 440% at 1.5 wt% ANFs [31].

Thus, it may be clearly deduced that within the many exemplified nanocomposites, nanoreinforcement leads to a very pronounced enhancement of fracture toughness of between tens to hundreds of %, with the maximum values of which being reached at extremely low loading percentages, commonly between 0.1 and 1.5% nanofiller.

This is in strong contrast with the effect of nanofillers on the tensile strength and modulus of nanocomposites, with the increase being much smaller compared to that of the fracture toughness. For example, the hereby calculated average values of the increase percentage of the tensile strength and the modulus in 34 different reported carbon nanofiber-reinforced epoxy nanocomposites [32] are only 17.3% (SD = 18.4) and 22.9% (SD = 27), respectively. It is also important to note that, for both the tensile strength and the modulus, the standard deviation is larger than the average value, which in this case stems from a decrease in these tensile properties in some of the nanocomposites (i.e., negative increase values) [32].

Nevertheless, as opposed to regular fillers, which do not enhance and mostly even decrease the ultimate strengths as compared with the pure matrix (while modulus and Tg are increased) [33], nanofillers mostly lead to an increase in both tensile strength and modulus, though a steady decrease is observed above approximately the same load thresholds of between 0.1 and 1.5%, as observed for the fracture toughness. This is most probably due to the agglomeration effect.

4. Effects of Agglomeration

Among the most dominant inherent properties of nanomaterials is their extremely high specific surface area. This property is most enhanced in two types of geometries: the first is a one-dimensional geometry, constituting of nanofibers, and the second is a

two-dimensional geometry, constituting nanoplates [34,35]. For example, some nanoclay minerals such as montmorillonite may reach a specific surface area of between 500 and 700 m^2/g [34–36].

Thus, theoretically, a very efficient reinforcing effect in nanocomposites would be expected. Nevertheless, this extremely high specific surface area of nanofillers also inherently produces very high attraction forces between nanoparticles and the abundant formation of interparticle physical bonds, thereby producing nanoparticles agglomerations and significantly reducing their interface with the matrix trough, which is where stress transfer would occur. Most agglomeration occurs during nanocomposite processing, resulting in nanofillers agglomerates with or without polymer matrix penetration [37–41].

Among the main approaches, which are abundantly researched and applied in an attempt of minimizing agglomeration, are various dispersion and exfoliation techniques (e.g., by sonication) and the surface coating or functionalization of the nanofillers—thus minimizing interparticle attraction and increasing particle–matrix compatibility and optimizing the processing parameters (e.g., extruder screw-related parameters). All attempted approaches do not completely prevent agglomeration and at least some agglomeration always exists in polymer nanocomposites [37–41]. Also, it was observed, for carbon nanotube-reinforced polymer nanocomposites, that agglomerates occurred despite functionalization and that cracks penetrated through the agglomerates into the matrix, thus not participating in resisting the crack and not contributing to enhancing fracture toughness [40,42].

5. Aspects of Polymer Chain Behavior and Interphase Formation

5.1. Chain Configuration

The main characteristic separating polymer nanocomposites from ceramic and metal nanocomposites is the fact that polymers consist of macromolecular chains of extremely high molecular weights, ranging from tens of thousands, to hundreds of thousands, and even to millions of g/mol. Consequently, in contrast to ceramic and metal matrices, the spatial configuration and orientation of the polymeric chains within the polymeric matrix constitutes a paramount factor affecting practically every aspect related to the final nanocomposite properties. As opposed to the average molecular weight and eventual degree of crosslinking (if present), which may be controlled via well-known mechanisms, local short-range and even overall long-range chain orientation within the polymer matrix are very difficult to control or prevent. This is mainly due to processing-related liquid polymer flow (of either the melt, or pre-crosslinked liquid), producing shear stresses that lead to polymer chain extension and orientation. This phenomenon results in inhomogeneities within the nanocomposite polymer matrix, affecting all physical and mechanical properties, including inhomogeneities in the crystallization of crystallizable polymeric matrices [43–46].

Although crosslinked polymeric matrices are commonly amorphous and the crosslinking process usually occurs under quiescent conditions in a mold, anisotropy may still occur due to chain orientation during pre-crosslinking flow-induced shear stresses the and crosslinking of the chains in an oriented chain-extended state. It was recently demonstrated in highly crosslinked segmented polyurethanes that the crosslinked networks are anchored in extended chain conformation, following pre-crosslinking stirring-related chain-orienting shear stresses [47]. This resulted in a significant anisotropic mechanical behavior, with enhanced properties in the oriented chain direction, and the significant chain-extended crystallization of otherwise non-crystallizable segments [47].

5.2. Interphases in Polymer Nanocomposites

Two different types of interphases are widely researched and reported as related to polymer nanocomposites.

The first type is the transcrystalline interphase, which is widely known in both polymeric composites [48–59] and polymeric nanocomposites [60–63] and can only be formed in crystallizable matrices.

Nanofibers and nanoparticles generally act as heterogeneous nucleating surfaces, inducing highly dense nuclei, which hinder the lateral extension of the crystals and force them to grow in one direction, outward from and normal to the nucleating nanofiller surface, resulting in oriented lamellar microstructures that constitute the transcrystalline layer interphase [60–63]. Single-fiber pull-out tests have demonstrated that the presence of a transcrystalline interphase significantly improves interfacial adhesion and stress transfer [60].

The second type of interphase is generally viewed as an ultrathin disordered layer surrounding each individual nanofiller (when ideally dispersed and distanced from each other), exhibiting different properties from bulk matrix and nanoparticles [45]. At the interface between the nanofillers and bulk polymers, the chain dynamics are reported to be different from those of the bulk polymer. The polymer chains, which adsorb to the nanofiller surface and accumulate near the surface, are relatively sparse and have an excess free volume [64–67]. Also, this adsorption is believed to be irreversible due to a supposedly required simultaneous desorption of all adsorbed segments [66]. However, it has also been argued that the adsorbed layers are not totally immobile under all circumstances [66]. It is suggested that the improvement in the polymer nanocomposites properties stems from the interphase formed between the nanofillers and bulk polymer matrix due to chain dynamics that are different from those of the bulk. The level and properties of the interphase are considered to predominantly affect the level of dissipated energy by different damaging mechanisms that occur at the nanoscale [64–67].

Nevertheless, the interphase cannot be experimentally characterized due to its very small thickness. Thus, the properties of the interphase could only be assessed by various modeling approaches. Accordingly, a multi-layered interphase was suggested to form in polymer nanocomposites. It was also assumed that each layer in the interphase possesses different properties [65].

The disordered state of this interphase, though, may be disputed in view of the above-discussed processing-related melt flow and the consequent polymer chain orientation due to the shear stresses induced by said flow. Thus, the processing-induced liquid-state matrix flow in the preparation of nanocomposites inevitably also occurs at the nanofiller–matrix interface.

It was demonstrated in a recent study [68] that processing-related melt flow against any interface—even at the interface with air (e.g., the interface with an entrapped air bubble or at the edges of the sample)—results in a shear stress-related chain orientation at said interfaces. It was also demonstrated [68] that a mechanism of self-shear chain orientation occurs as a consequence of crystal growth within the polymer melt. It was shown that this probably inevitable chain orientation at interfaces induces the heterogeneous nucleation of transcrystalline interphases thereon and is also the mechanism by which banded spherulites are formed [68]. This was also in strong agreement with a previous study suggesting a similar shear orientation mechanism at the melt–crystalline interface [69].

Thus, it is highly possible that the above-described interphase, commonly considered as disordered [64–67], may actually be significantly ordered and at least partially chain-oriented. This is also highly consistent with research reporting the development of a transcrystalline interphase on nanofillers [60–63], since a transcrystalline interphase cannot be heterogeneously nucleated on disordered polymer chains—only on oriented chains [70].

It may also be deduced here that the various types of anisotropy and inhomogeneities in the polymer matrix influencing the development and properties of the interphases in nanocomposites may also at least partially determine crack propagation directions and pinning—thus significantly affecting the fracture toughness of polymer nanocomposites.

6. Nano-Geometrical and Atomic-Scale Effects

In terms of the interaction occurring at the interface between the polymeric matrix and nanofillers, under an applied stress, various experimental and modeling approaches relate

to the nano-geometry of nanofillers—particularly carbon nanotubes—and the atomic-scale bonds and interactions therewith.

It was demonstrated that the load transfer efficiency of carbon nanotubes (CNTs) directly depends on the atomic interface interaction with polymeric matrix molecules, which is mostly very weak, in view of the high crystallinity of CNTs that renders them inert [71]. The use of helical CNTs—exhibiting a helical nano-geometry—was shown to be mechanically interlocked within the polymer matrix in polymeric nanocomposites [72]. It was also demonstrated, that although their interface atomic bonding with polymeric matrix molecules was weak, they exhibited strong pull-out resistance and efficient load transfer when subjected to external loads [72]. Accordingly, a significant maximum increase in fracture toughness of 31% was obtained with only 0.05% of helical CNTs, while approximately the same maximum increase in fracture toughness was obtained with double the loading fraction, i.e., 0.1% of straight CNTs, as compared to the pristine epoxy matrix [72]. It was also reported [73] that the coiled CNT polyethylene nanocomposite exhibited a higher energy absorption capability than the CNT-reinforced polyethylene nanocomposite. Accordingly, at a load fraction of 1%, nanocomposite fracture toughness was only 1.012 MJ/m^3 with straight CNTs and 1.842 MJ/m^3 with coiled CNTs [73].

Computational studies are mostly based on both atomistic techniques such as molecular dynamics and continuum-based shell and beam models [74]. Also investigated was the applicability of continuum models by comparison to molecular dynamics simulations [75]. Analytical expressions were presented for nanotubes and multiwall nanotubes, with shells interacting through Van Der Wall forces [76,77]. The role of atomic scale interfaces in the load transfer characteristics of nanotubes, as related to the compressive behavior of CNT-reinforced nanocomposites, were investigated [78]. It was shown that in the post-buckling stage, the nanotubes behave like short fibers and deform via crushing. Comparing with the results of continuum solutions, it was concluded that the continuum solutions should be applied cautiously as related to nanoscale interfaces [78].

7. Theoretical Investigations of Fracture Toughness

As hereby exemplified, a vast number of experimental studies have reported additional energy dissipation due to factors that include interfacial debonding, formation of shear bands around nanoparticles, crack propagation mechanisms, etc., occurring as macroscale fractures, which progress in nanocomposites as main mechanisms that improve fracture toughness. Thus, crack propagation in nanocomposites is increasingly viewed by some recent modeling studies as a multiscale system consisting of simultaneous macroscale fractures and nano/microscale energy dissipation [79,80]. Multiscale models were developed and suggested for CNT-reinforced nanocomposites, related to the main mechanisms of pull-out of carbon nanotube [81], interfacial debonding of the CNTs [82], and plastic void growth [83]. Multiscale models that include the possibility of CNT rupture were also suggested [84,85].

8. Interlayer Nanoreinforcements of Polymer Composites

Although laminate composites have many distinct advantages over conventional materials due to their excellent corrosion resistance, low density, and high specific modulus and strength [86], they are highly susceptible to interfacial damage [87], resulting in very poor out-of-plane transversal and in-plane shear performance [88–90].

The interlaminar properties of laminate composites depend exclusively on the characteristics of the matrix and interface, thus exhibiting significant weakness under conditions that generate shear stresses—e.g., under static or dynamic flexure. These shear stresses develop at the midplane of the laminate, eventually causing interlaminar failure. Consequently, improving the mechanical properties in general and particularly the interlaminar fracture toughness is among the most investigated aspects in the field of polymer composites.

Delamination was reported to be the main failure mechanism of carbon fiber-reinforced polymer laminate composites, significantly reducing their strength and stiffness, which can be of catastrophic consequences, especially in the aerospace industry [91]. Said delamination failure process being mainly attributed to the lack of through-thickness fiber reinforcement, hence the interlaminar regions are virtually governed by the brittle epoxy resin matrix [91].

Various possible solutions were investigated in an attempt to mitigate these deficiencies by z-directional reinforcement, for example, z-pinning [92] and 3D stitched or woven fibers [93]. Nevertheless, the in-plane mechanical properties of the laminated composites may consequently be compromised by frequently occurring fracture, crimping, and misalignment of the reinforcing fibers [94].

It was demonstrated in relatively early studies [95,96] that interlaminar fracture toughness can be significantly improved with the addition of extremely small amounts of carbon nanotubes, without significantly compromising the in-plane laminate mechanical properties [94,96].

Interleaving is an extensively researched method, which focuses on the interlaminar midplane, and consists of the selective placement of a leaf of nano-reinforced polymer at the midplane of the laminated composite, instead of mixing an equivalent load of nanoparticles throughout the matrix. This concept was shown to provide a relatively simple and significantly effective means of interfacial toughening, without changing the prepreg processing, by matrix modification using, for example, non-woven fiber veils [97–99], carbon nanotubes [100], and graphene [101]. The advantages of nano-reinforced interleaving include being considerably more cost-effective method since nanofillers are not wastefully dispersed throughout the entire matrix, but confined to a selective region where the maximum shear stresses are expected to occur. Thus, significantly smaller loads of nanofiller are required to obtain the same improvement in fracture toughness with lesser effects on the laminate in-plane mechanical properties.

Although a thicker interlayer was demonstrated to significantly improve the fracture toughness of laminate composites using various nanofillers-containing interlayers [102–104], it has the disadvantage of reducing the overall volume fraction of carbon fibers, thus impairing the in-plane strength of the laminate composites [102–104].

A z-directional nanoreinforcement was used, attempting to mitigate the poor in-plane shear and out-of-plane response of glass fiber–epoxy laminate composites under extreme temperature conditions via the dispersion of either functionalized or non-functionalized carbon nanotubes within the epoxy matrix and applying a z-direction electric field alignment treatment, resulting in an improvement of up to 47% in flexural strength compared to the control laminate [105].

A study of the Mode I fracture toughness of polyethylene fibers and polyurethane matrix composite laminates interleaved with thin polyurethane films with either untreated or functionalized carbon nanotubes [106] showed a significant improvement of the Mode I initiation and propagation fracture toughness, compared to the non-interleaved laminates and laminates interleaved with unreinforced polyurethane films [106].

Woven carbon fiber/epoxy laminates, interleaved with 0.5% SP1 protein-treated carbon nanotube-reinforced epoxy nanocomposite thin leaves, were tested for Mode II interlaminar fracture toughness and interlaminar shear strength [107]. The SP1 protein functionalization was used in view of its ability to simultaneously bind to the carbon nanotubes and to the epoxy matrix. An 85% improvement in the interlaminar fracture toughness was obtained, without deteriorating the interlaminar shear strength [107].

Similar interleaved laminate composites, as in reference [107], were tested under dynamic conditions [4]. The fracture properties were measured by the crack lap shear method at two different loading rates, i.e., at 4 m/s and 8 m/s. It was demonstrated that since the fracture toughness is sensitive to crack velocity, which in turn is determined by the loading rate, fracture toughness is significantly higher at high crack velocities by becoming more sensitive to the energy dissipation mechanisms of crack front interactions [4]. Mode II

interlaminar fracture toughness improvements for both the crack initiation and propagation phases reached up to 145% for certain dynamic loading conditions [4].

Carbon fiber laminate hybridization with glass fibers is often suggested and investigated with the purpose of lowering the very costly carbon fiber content [108]. Nevertheless, longitudinal delamination at the fiber interface was reported to occur due the significant difference in the elongation behavior of these fiber types [108].

Veil interleaving was intensively investigated for inducing pseudo-ductility—i.e., reorientation of fibers under strain, thereby achieving a higher failure strain and nonlinear behavior—to reduce the delamination and buckling that lead to premature failure in hybrid laminates. For example, a pseudo-ductile response was obtained with hybrid carbon/E-glass fibers laminate composites, interlayered by Nylon 6,6 nanofiber veils, thereby a 24% increase in the strain at failure was obtained, along with a significant reduction in buckling failure [109]. Also, for hybrid carbon/glass fiber composites, interlayered with Nylon 6,6 nanofiber veils under three-point bending cyclic loading, an improved flexural modulus retention of 66.87% and a 10-fold increase in fatigue life was observed compared with the non-veiled controls [110].

Nylon 6,6 nanofiber-reinforced veils in carbon fiber-reinforced polymer laminates, exhibited an increase in fracture toughness for Mode I crack opening by 150% and Mode II by 50% [111]. Also, the matrix cracking was reduced by 92% for a similar laminate using electrospun nylon 6,6 nanofiber-reinforced veils [112].

9. Conclusions

Based on the examples above of various nanocomposites, it is concluded that nanoparticles of different shapes and geometries—even at relatively low concentrations—improve fracture toughness significantly in comparison with the pristine polymers. The improvements stem from the ability of nanoparticles to interact with the advancing crack front via various mechanisms (e.g., fiber pull-out and crack front bowing), thereby slowing down or arresting its propagation.

Author Contributions: The two authors contributed equally to the literature survey and the writing of the article. All authors have read and agreed to the published version of the manuscript.

Funding: This research received no external funding.

Data Availability Statement: No new data were created or analyzed in this study.

Conflicts of Interest: The authors declare no conflict of interest.

References

1. Stern, N.; Marom, G.; Zhang, L.; Hu, X. Micromechanics of Nanocomposites. In *Comprehensive Composite Materials II*; Beaumont, P.W.R., Zweben, C.H., Eds.; Academic Press: Oxford, UK, 2018; Volume 6, pp. 1–27.
2. Marom, G.; Wagner, H.D. Should polymer nanocomposites be regarded as molecular composites? *J. Mater. Sci.* **2017**, *52*, 8357–8361. [CrossRef]
3. Marom, G.; Wagner, H.D. A perspective on the structure and properties of nanocomposites. *Polym. Compos.* **2020**, *41*, 2986–2989. [CrossRef]
4. Lyashenko-Miller, T.; Fitoussi, J.; Marom, G. The loading rate effect on Mode II fracture toughness of composites interleaved with CNT nanocomposites. *Nanocomposites* **2016**, *2*, 1–7. [CrossRef]
5. Lange, F. The interaction of a crack front with a second-phase dispersion. *Philos. Mag.* **1970**, *22*, 0983–0992. [CrossRef]
6. Day, R.J.; Lovell, P.A.; Wazzan, A.A. Toughened carbon/epoxy composites made by using core/shell particles. *Compos. Sci. Tech.* **2001**, *61*, 41–56. [CrossRef]
7. Domun, N.; Hadavinia, H.; Zhang, T.; Sainsbury, T.; Liaghata, G.H.; Vahid, S. Improving the fracture toughness and the strength of epoxy using nanomaterials—A review of the current status. *Nanoscale* **2015**, *7*, 10294–10329. [CrossRef]
8. Xiao, Q.; Dai, M.; Huang, M.; Lim, L.T. Bioinspired pullulan-starch nanoplatelets nanocomposite films with enhanced mechanical properties. *Carbohydr. Polym.* **2024**, *329*, 121769. [CrossRef]
9. George, J.S.; Vahabi, H.; Maria, H.J.; Anju, C.S.; Thomas, S. Sustainable hybrid green nanofiller based on cellulose nanofiber for enhancing the properties of epoxy resin. *Colloids Surf. A Physicochem. Eng. Asp.* **2024**, *694*, 134082. [CrossRef]
10. Stojanović, D.B.; Brajović, L.; Obradović, V.; Mijailović, D.; Dramlić, D.; Kojović, A.; Uskoković, P.S. Hybrid acrylic nanocomposites with excellent transparency and hardness/toughness balance. *Prog. Org. Coat.* **2020**, *139*, 105437. [CrossRef]

11. Zhang, H.; Chen, J.; Zhou, S.; Jing, J.; Fu, J. A nacre-inspired thermo conductive and healable nanocomposite captures extremely enhanced stiffness and toughness. *Compos. Part B Eng.* **2024**, *272*, 111228. [CrossRef]
12. Dong, M.; Tomes, O.; Soul, A.; Hu, Y.; Bilotti, E.; Zhang, H.; Papageorgiou, D.G. Hybrid Ti3C2T x MXene and Carbon Nanotube Reinforced Epoxy Nanocomposites for Self-Sensing and Structural Health Monitoring. *ACS Appl. Nano Mater.* **2024**, *7*, 3314–3325. [CrossRef]
13. Wang, H.; Lu, R.; Li, L.; Liang, C.; Yan, J.; Liang, R.; Sun, G.; Jiang, L.; Cheng, Q. Strong, tough, and thermally conductive nacre-inspired boron nitride nanosheet/epoxy layered nanocomposites. *Nano Res.* **2024**, *17*, 820–828. [CrossRef]
14. Chung, S.; Park, S.A.; Park, S.B.; Kwak, H.; Oh, D.X.; Hwang, D.S.; Jeon, H.; Koo, J.M.; Park, J. Biobased super engineering plastic nanocomposite of cellulose nanofibers and isosorbide. *Polym. Degrad. Stab.* **2023**, *215*, 110445. [CrossRef]
15. Alam, M.N.; Kumar, V.; Lee, D.J.; Choi, J. Synergistically toughened silicone rubber nanocomposites using carbon nanotubes and molybdenum disulfide for stretchable strain sensors. *Compos. Part B Eng.* **2023**, *259*, 110759. [CrossRef]
16. Tiwari, A. Nanocomposite fracture analysis: Aligned Fe3O4-GNP nanoplatelets' effects on KIC, GIC, CTODc, and fracture mechanisms in epoxy matrices. *Compos. Struct.* **2024**, *341*, 118208. [CrossRef]
17. Kumari, S.; Hussain, A.; Rao, J.; Singh, K.; Avinashi, S.K.; Gautam, C. Structural, mechanical and biological properties of PMMA-ZrO2 nanocomposites for denture applications. *Mater. Chem. Phys.* **2023**, *295*, 127089. [CrossRef]
18. Kexuan, S.; Xu, W.; Wu, N.; Ouyang, S. Mussel-Inspired Renewable and High-Performance Montmorillonite-Based Composites with a "Brick-and-Mortar" Structure. *J. Polym. Environ.* **2023**, *31*, 3081–3093. [CrossRef]
19. Ma, Q.; Hao, B.; Ma, P.C. In-situ characterization on the fracture behavior of three-dimensional polymer nanocomposites reinforced by CNT sponge. *Compos. Sci. Technol.* **2022**, *217*, 109132. [CrossRef]
20. Li, X.; Wang, Q.; Cui, X.; Feng, X.; Teng, F.; Xu, M.; Su, W.; He, J. Study on the mechanical and toughness behavior of epoxy nano-composites with zero-dimensional and two-dimensional nano-fillers. *Polymers* **2022**, *14*, 3618. [CrossRef]
21. Sarath Kumar, P.; Jayanarayanan, K.; Deeraj, B.D.S.; Joseph, K.; Balachandran, M. Synergistic effect of carbon fabric and multiwalled carbon nanotubes on the fracture, wear and dynamic load response of epoxy-based multiscale composites. *Polym. Bull.* **2022**, *79*, 5063–5084. [CrossRef]
22. Ma, H.; Aravand, M.A.; Falzon, B.G. Synergistic enhancement of fracture toughness in multiphase epoxy matrices modified by thermoplastic and carbon nanotubes. *Compos. Sci. Technol.* **2021**, *201*, 108523. [CrossRef]
23. Sahu, M.; Narasimhan, L.; Raichur, A.M.; Sover, A.; Ciobanu, R.C.; Lucanu, N.; Aradoaei, M. Improving fracture toughness of tetrafunctional epoxy with functionalized 2D molybdenum disulfide nanosheets. *Polymers* **2021**, *13*, 4440. [CrossRef] [PubMed]
24. Dungani, R.; Sumardi, I.; Alamsyah, E.M.; Aditiawati, P.; Karliati, T.; Malik, J.; Sulistyono. A study on fracture toughness of nano-structured carbon black-filled epoxy composites. *Polym. Bull.* **2021**, *78*, 6867–6885. [CrossRef]
25. Kim, S.H.; Rhee, K.Y.; Park, S.J. Amine-terminated chain-grafted nanodiamond/epoxy nanocomposites as interfacial materials: Thermal conductivity and fracture resistance. *Compos. Part B Eng.* **2020**, *192*, 107983. [CrossRef]
26. Soudmand, B.H.; Shelesh-Nezhad, K.; Hassanifard, S. Toughness evaluation of poly (butylene terephthalate) nanocomposites. *Theor. Appl. Fract. Mech.* **2020**, *108*, 102662. [CrossRef]
27. Mirzapour, M.; Robert, M.; Benmokrane, B. In Situ Processing to Achieve High-Performance Epoxy Nanocomposites with Low Graphene Oxide Loading. *C* **2024**, *10*, 52. [CrossRef]
28. Chaeichian, S.; Wood-Adams, P.M.; Hoa, S.V. Effect of morphology on fracture toughness of unsaturated polyester-based hybrid nanocomposites. *Polymer* **2015**, *72*, 154–164. [CrossRef]
29. Jung, J.; Sodano, H.A. Cellulose nanocrystal functionalized aramid nanofiber reinforced epoxy nanocomposites with high strength and toughness. *Nanotechnology* **2023**, *34*, 245703. [CrossRef]
30. Yu, T.; Zhu, F.; Peng, X.; Chen, Z. Acetylated Nanocelluloses Reinforced Shape Memory Epoxy with Enhanced Mechanical Properties and Outstanding Shape Memory Effect. *Nanomaterials* **2022**, *12*, 4129. [CrossRef]
31. Jung, J.; Sodano, H.A. High strength epoxy nanocomposites reinforced by epoxy functionalized aramid nanofibers. *Polymer* **2020**, *195*, 122438. [CrossRef]
32. Santos, P.; Silva, A.P.; Reis, P.N. The Effect of Carbon Nanofibers on the Mechanical Performance of Epoxy-Based Composites: A Review. *Polymers* **2024**, *16*, 2152. [CrossRef]
33. Matthews, F.L.; Rawlings, R.D. *Composite Materials: Engineering and Science*; CRC Press: Boca Raton, FL, USA; Woodhead Publishing Limited: Cambridge, UK, 2006.
34. Horniak, G.L.; Tibbals, H.F.; Dutta, J.; Moore, J.J. *Introduction to Nanoscience & Nanotechnology*; CRC Press: New York, NY, USA; Taylor & Francis Group: Abingdon, UK, 2009.
35. Ozin, G.A.; Arsenault, A.C.; Cademartiri, L. *Nanochemistry, A Chemical Approach to Nanomaterials*; RSC Publishing: Cambridge, UK, 2009.
36. Van Olphen, H. *An Introduction to Clay Colloid Chemistry*; Interscience Publishers: New York, NY, USA, 1964.
37. Zare, Y. Study of nanoparticles aggregation/agglomeration in polymer particulate nanocomposites by mechanical properties. *Compos. Part A Appl. Sci. Manuf.* **2016**, *84*, 158–164. [CrossRef]
38. Kumar, S. Investigating effect of CNT agglomeration in CNT/polymer nanocomposites using multiscale finite element method. *Mech. Mater.* **2023**, *183*, 104706. [CrossRef]
39. Ma, X.; Zare, Y.; Rhee, K.Y. A two-step methodology to study the influence of aggregation/agglomeration of nanoparticles on Young's modulus of polymer nanocomposites. *Nanoscale Res. Lett.* **2017**, *12*, 621. [CrossRef] [PubMed]

40. Abhiram, B.R.; Ghosh, D. Influence of nanofiller agglomeration on fracture properties of polymer nanocomposite: Insights from atomistic simulation. *Eng. Fract. Mech.* **2023**, *290*, 109503.
41. Du, H.; Zhang, J.; Fang, C.; Weng, G.J. Modeling the evolution of graphene agglomeration and the electrical and mechanical properties of graphene/polypropylene nanocomposites. *J. Appl. Polym. Sci.* **2023**, *140*, 53292. [CrossRef]
42. Hsieh, T.H.; Kinloch, A.J.; Taylor, A.C.; Kinloch, I.A. The effect of carbon nanotubes on the fracture toughness and fatigue performance of a thermosetting epoxy polymer. *J. Mater. Sci.* **2011**, *46*, 7525–7535. [CrossRef]
43. Bower, D.I. *Introduction to Polymer Physics*; Cambridge University Press: Cambridge, UK, 2008.
44. Sommer, J.U.; Reiter, G. (Eds.) *Polymer Crystallization—Observations, Concepts and Interpretations*; Lecture Notes in Physics; Springer: Berlin, Germany, 2003.
45. Liu, Q.; Sun, X.; Li, H.; Yan, S. Orientation-induced crystallization of isotactic polypropylene. *Polymer* **2013**, *54*, 4404–4421. [CrossRef]
46. Hu, W. Personal perspective on strain-induced polymer crystallization. *J. Phys. Chem. B* **2023**, *127*, 822–827. [CrossRef]
47. Stern, T. Single-Step Synthesis and Characterization of Non-Linear Tough and Strong Segmented Polyurethane Elastomer Consisting of Very Short Hard and Soft Segments and Hierarchical Side-Reacted Networks and Single-Step Synthesis of Hierarchical Hyper-Branched Polyurethane. *Molecules* **2024**, *29*, 1420. [CrossRef]
48. Stern, T.; Wachtel, E.; Marom, G. Origin, Morphology and Crystallography of Transcrystallinity in Polyethylene-Based Single Polymer Composites. *Compos. Part A Appl. Sci. Manuf.* **1997**, *28*, 437–444. [CrossRef]
49. Quan, H.; Li, Z.-M.; Yang, M.-B.; Huang, R. On transcrystallinity in semi-crystalline polymer composites. *Compos. Sci. Technol.* **2005**, *65*, 999–1021. [CrossRef]
50. Liang, Y.; Zheng, G.; Liu, S.; Dai, K.; Liu, C.; Chen, J.; Shen, C. β-Crystal in the iPP melt encapsulated by transcrystallinity and spherulites: Effect of molecular weight. *J. Mater. Sci.* **2013**, *48*, 2326–2333. [CrossRef]
51. Billon, N.; Magnet, C.; Haudin, J.M.; Lefebvre, D. Transcrystallinity effects in thin polymer films. Experimental and theoretical approach. *Colloid Polym. Sci.* **1994**, *272*, 633–654. [CrossRef]
52. Li, C.; Gao, Y.; Wang, L.; Li, J.; Guo, S. Fabrication, structure, and properties of Poly-(Lactide) multilayers with ultrahigh content, ordered, and continuous transcrystallinity. *Polymer* **2021**, *228*, 123933. [CrossRef]
53. Stern, T.; Teishev, A.; Marom, G.; Varelidis, P.C.; Papaspyrides, C.D. Processing of Composites of Chopped PE Fiber-Reinforced PE Matrix. *Adv. Compos. Lett.* **1996**, *5*, 103–106.
54. Stern, T.; Teishev, A.; Marom, G. Composites of Polyethylene Reinforced with Chopped Polyethylene Fibers: Effect of Transcrystalline Interphase. *Compos. Sci. Technol.* **1997**, *57*, 1009–1015. [CrossRef]
55. Stern, T.; Wachtel, E.; Marom, G. Epitaxy and Lamellar Twisting in Transcrystalline Polyethylene. *J. Polym. Sci. Part B Polym. Phys.* **1997**, *35*, 2429–2433. [CrossRef]
56. Zafeiropoulos, N.E.; Papaspyrides, C.D.; Varelidis, P.C.; Stern, T.; Marom, G. Characterization of Coatings of LDPE Residual Matrix Deposited on Glass Fibers by a Dissolution/Reprecipitation Recycling Process. *Compos. Part A Appl. Sci. Manuf.* **1999**, *30*, 831–838. [CrossRef]
57. Zhang, S.; Minus, M.L.; Zhu, L.; Wong, C.P.; Kumar, S. Polymer transcrystallinity induced by carbon nanotubes. *Polymer* **2008**, *49*, 1356–1364. [CrossRef]
58. Lenes, M.; Gregersen, Ø.W. Effect of surface chemistry and topography of sulphite fibres on the transcrystallinity of polypropylene. *Cellulose* **2006**, *13*, 345–355. [CrossRef]
59. Karger-Kocsis, J. Interphase with Lamellar Interlocking and Amorphous Adherent—A Model to Explain Effects of Transcrystallinity. *Adv. Compos. Lett.* **2000**, *9*, 96369350000900. [CrossRef]
60. Abdou, J.P.; Reynolds, K.J.; Pfau, M.R.; van Staden, J.; Braggin, G.A.; Tajaddod, N.; Minus, M.; Reguero, V.; Vilatela, J.J.; Zhang, S. Interfacial crystallization of isotactic polypropylene surrounding macroscopic carbon nanotube and graphene fibers. *Polymer* **2016**, *91*, 136–145. [CrossRef]
61. Liang, Y.; Liu, S.; Dai, K.; Wang, B.; Shao, C.; Zhang, Q.; Wang, S.; Zheng, G.; Liu, C.; Chen, J.; et al. Transcrystallization in nanofiber bundle/isotactic polypropylene composites: Effect of matrix molecular weight. *Colloid Polym. Sci.* **2012**, *290*, 1157–1164. [CrossRef]
62. Cho, B.G.; Lee, J.E.; Hwang, S.H.; Han, J.H.; Chae, H.G.; Park, Y.B. Enhancement in mechanical properties of polyamide 66-carbon fiber composites containing graphene oxide-carbon nanotube hybrid nanofillers synthesized through in situ interfacial polymerization. *Compos. Part A Appl. Sci. Manuf.* **2020**, *135*, 105938. [CrossRef]
63. Karevan, M.; Kalaitzidou, K. Formation of a complex constrained region at the graphite nanoplatelets-polyamide 12 interface. *Polymer* **2013**, *54*, 3691–3698. [CrossRef]
64. Zare, Y.; Rhee, K.Y. A simple technique for calculation of an interphase parameter and interphase modulus for multilayered interphase region in polymer nanocomposites via modeling of young's modulus. *Phys. Mesomech.* **2020**, *23*, 332–339. [CrossRef]
65. Zare, Y.; Rhee, K.Y. Dependence of Z parameter for tensile strength of multi-layered interphase in polymer nanocomposites to material and interphase properties. *Nanoscale Res. Lett.* **2017**, *12*, 42. [CrossRef]
66. Huang, J.; Zhou, J.; Liu, M. Interphase in polymer nanocomposites. *JACS Au* **2022**, *2*, 280–291. [CrossRef]
67. Brent Strong, A. *Plastics—Materials and Processing*; Prentice Hall: Upper Saddle River, NJ, USA, 1996.
68. Stern, T. Transcrystalline Mechanism of Banded Spherulites Development in Melt-Crystallized Semicrystalline Polymers. *Polymers* **2024**, *16*, 2411. [CrossRef]

69. Stern, T. Polymeric Micro-Sequential Concentric Transcrystalline Morphology Self-Assembly, with Intermittent Self-Shear-Oriented Amorphous Layers. *Polym. Adv. Technol.* **2017**, *28*, 1670–1675. [CrossRef]
70. Su, F.; Ji, Y.; Meng, L.; Chang, J.; Chen, L.; Li, L. Shear-induced precursors in polyethylene: An in-situ synchrotron radiation scanning X-ray microdiffraction study. *Polymer* **2018**, *135*, 61–68. [CrossRef]
71. Yao, X.; Gao, X.; Jiang, J.; Xu, C.; Deng, C.; Wang, J. Comparison of carbon nanotubes and graphene oxide coated carbon fiber for improving the interfacial properties of carbon fiber/epoxy composites. *Compos. Part B Eng.* **2018**, *132*, 170–177. [CrossRef]
72. Vijayan, R.; Ghazinezami, A.; Taklimi, S.R.; Khan, M.Y.; Askari, D. The geometrical advantages of helical carbon nanotubes for high-performance multifunctional polymeric nanocomposites. *Compos. Part B Eng.* **2019**, *156*, 28–42. [CrossRef]
73. Yousefi, E.; Sheidaei, A.; Mahdavi, M.; Baniassadi, M.; Baghani, M.; Faraji, G. Effect of nanofiller geometry on the energy absorption capability of coiled carbon nanotube composite material. *Compos. Sci. Technol.* **2017**, *153*, 222–231. [CrossRef]
74. Nardelli, M.B.; Yakobson, B.I.; Bernholc, J. Mechanism of strain release in carbon nanotubes. *Phys. Rev. B* **1998**, *57*, R4277. [CrossRef]
75. Harik, V.M. Mechanics of carbon nanotubes: Applicability of the continuum-beam models. *Comput. Mater. Sci.* **2002**, *24*, 328–342. [CrossRef]
76. Ru, C.Q. Effect of van der Waals forces on axial buckling of a double-walled carbon nanotube. *J. Appl. Phys.* **2000**, *87*, 7227–7231. [CrossRef]
77. Ru, C.Q. Axially compressed buckling of a doublewalled carbon nanotube embedded in an elastic medium. *J. Mech. Phys. Solids* **2001**, *49*, 1265–1279. [CrossRef]
78. Namilae, S.; Chandra, N. Role of atomic scale interfaces in the compressive behavior of carbon nanotubes in composites. *Compos. Sci. Technol.* **2006**, *66*, 2030–2038. [CrossRef]
79. Lee, J.; Wang, H.; Kim, J.H.; Shin, H. Recent studies on the multiscale modeling and simulation of polymer nanocomposites. *JMST Adv.* **2023**, *5*, 85–91. [CrossRef]
80. Wang, H.; Shin, H. Recent studies on the multiscale models for predicting fracture toughness of polymer nanocomposites. *Multiscale Sci. Eng.* **2022**, *4*, 1–9. [CrossRef]
81. Lachman, N.; Wagner, H.D. Correlation between interfacial molecular structure and mechanics in CNT/epoxy nano-composites. *Compos. Part A Appl. Sci. Manuf.* **2010**, *41*, 1093–1098. [CrossRef]
82. Shokrieh, M.M.; Zeinedini, A. Effect of CNTs debonding on mode I fracture toughness of polymeric nanocomposites. *Mater. Des.* **2016**, *101*, 56–65. [CrossRef]
83. Shin, H. Multiscale model to predict fracture toughness of CNT/epoxy nanocomposites. *Compos. Struct.* **2021**, *272*, 114236. [CrossRef]
84. Mirjalili, V.; Hubert, P. Modelling of the carbon nanotube bridging effect on the toughening of polymers and experimental verification. *Compos. Sci. Technol.* **2010**, *70*, 1537–1543. [CrossRef]
85. Wang, H.; Lee, J.; Kim, J.H.; Shin, H. Multiscale strategy to predict the fracture toughness and crack extension behavior of ozone-functionalized carbon nanotube/epoxy nanocomposites. *Chem. Eng. J.* **2023**, *465*, 142985. [CrossRef]
86. Hollaway, L.C. A review of the present and future utilization of FRP composites in the civil infrastructure with reference to their important in-service properties. *Constr. Build. Mater.* **2010**, *24*, 2419–2445. [CrossRef]
87. Chen, D.; Luo, Q.; Meng, M.; Li, Q.; Sun, G. Low velocity impact behavior of interlayer hybrid composite laminates with carbon/glass/basalt fibres. *Compos. Part B Eng.* **2019**, *176*, 107191. [CrossRef]
88. Mirjalili, V.; Ramachandramoorthy, R.; Hubert, P. Enhancement of fracture toughness of carbon fiber laminated composites using multi wall carbon nanotubes. *Carbon* **2014**, *79*, 413–423. [CrossRef]
89. Waqas, M.; Robert, C.; Arif, U.; Radacsi, N.; Ray, D.; Koutsos, V. Improving the through-thickness electrical conductivity of carbon fiber reinforced polymer composites using interleaving conducting veils. *J. Appl. Polym. Sci.* **2022**, *139*, e53060. [CrossRef]
90. Ozdemir, N.G. Toughening of carbon fibre reinforced polymer composites with rubber nanoparticles for advanced industrial applications. *Express Polym. Lett.* **2016**, *10*, 394–407. [CrossRef]
91. Towsyfyan, H.; Biguri, A.; Boardman, R.; Blumensath, T. Successes and challenges in non-destructive testing of aircraft composite structures. *Chin. J. Aeronaut.* **2020**, *33*, 771–791. [CrossRef]
92. Pingkarawat, K.; Mouritz, A.P. Comparative study of metal and composite z-pins for delamination fracture and fatigue strengthening of composites. *Eng. Fract. Mech.* **2016**, *154*, 180–190. [CrossRef]
93. Dransfield, K.A.; Jain, L.K.; Mai, Y.W. On the effects of stitching in CFRPs—I. Mode I delamination toughness. *Compos. Sci. Technol.* **1998**, *58*, 815–827. [CrossRef]
94. Mouritz, A.P.; Cox, B.N. A mechanistic interpretation of the comparative in-plane mechanical properties of 3D woven, stitched and pinned composites. *Compos. Part A Appl. Sci. Manuf.* **2010**, *41*, 709–728. [CrossRef]
95. Gojny, F.H.; Wichmann, M.H.G.; Köpke, U.; Fiedler, B.; Schulte, K. Carbon nanotube-reinforced epoxy-composites: Enhanced stiffness and fracture toughness at low nanotube content. *Compos. Sci. Technol.* **2004**, *64*, 2363–2371. [CrossRef]
96. Li, Y.; Hori, N.; Arai, M.; Hu, N.; Liu, Y.; Fukunaga, H. Improvement of interlaminar mechanical properties of CFRP laminates using VGCF. *Compos. Part A Appl. Sci. Manuf.* **2009**, *40*, 2004–2012. [CrossRef]
97. Yuan, B.; Tan, B.; Hu, Y.; Shaw, J.; Hu, X. Improving impact resistance and residual compressive strength of carbon fibre composites using un-bonded non-woven short aramid fibre veil. *Compos. Part A Appl. Sci. Manuf.* **2019**, *121*, 439–448. [CrossRef]

98. Ou, Y.; González, C.; Vilatela, J.J. Understanding interlaminar toughening of unidirectional CFRP laminates with carbon nanotube veils. *Compos. Part B Eng.* **2020**, *201*, 108372. [CrossRef]
99. Ou, Y.; González, C.; Vilatela, J.J. Interlaminar toughening in structural carbon fiber/epoxy composites interleaved with carbon nanotube veils. *Compos. Part A Appl. Sci. Manuf.* **2019**, *124*, 105477. [CrossRef]
100. He, Y.; Zhang, J.; Yao, L.; Tang, J.; Che, B.; Ju, S.; Jiang, D. A multi-layer resin film infusion process to control CNTs distribution and alignment for improving CFRP interlaminar fracture toughness. *Compos. Struct.* **2021**, *260*, 113510. [CrossRef]
101. Körbelin, J.; Kötter, B.; Voormann, H.; Brandenburg, L.; Selz, S.; Fiedler, B. Damage tolerance of few-layer graphene modified CFRP: From thin-to thick-ply laminates. *Compos. Sci. Technol.* **2021**, *209*, 108765. [CrossRef]
102. Hu, Y.; Wei, Y.; Han, G.; Zhang, J.; Sun, G.; Hu, X.; Cheng, F. Comparison of impact resistance of carbon fibre composites with multiple ultra-thin CNT, aramid pulp, PBO and graphene interlayers. *Compos. Part A Appl. Sci. Manuf.* **2022**, *155*, 106815. [CrossRef]
103. Zhang, J.; Lin, T.; Wang, X. Electrospun nanofibre toughened carbon/epoxy composites: Effects of polyetherketone cardo (PEK-C) nanofibre diameter and interlayer thickness. *Compos. Sci. Technol.* **2010**, *70*, 1660–1666. [CrossRef]
104. García-Rodríguez, S.M.; Costa, J.; Rankin, K.E.; Boardman, R.P.; Singery, V.; Mayugo, J.A. Interleaving light veils to minimise the trade-off between mode-I interlaminar fracture toughness and in-plane properties. *Compos. Part A Appl. Sci. Manuf.* **2020**, *128*, 105659. [CrossRef]
105. Fulmali, A.O.; Patnaik, S.; Rathore, D.K.; Bhattacharjee, D.; Gwalani, B.; Ray, B.C.; Prusty, R.K. Enhanced extreme temperature bending and delamination resistance of GFRP composites through z-directional aligned nano-reinforcement: Emphasizing the effects of CNT functionalization. *Compos. Sci. Technol.* **2023**, *244*, 110272. [CrossRef]
106. Lyashenko-Miller, T.; Marom, G. Delamination fracture toughness of UHMWPE fibers/polyurethane laminates interleaved with carbon nanotube-reinforced polyurethane films. *Polym. Adv. Technol.* **2017**, *28*, 606–612. [CrossRef]
107. Lyashenko, T.; Lerman, N.; Wolf, A.; Harel, H.; Marom, G. Improved Mode II delamination fracture toughness of composite materials by selective placement of protein-surface treated CNT. *Compos. Sci. Technol.* **2013**, *85*, 29–35. [CrossRef]
108. Ravishankar, B.; Nayak, S.K.; Kader, M.A. Hybrid composites for automotive applications—A review. *J. Reinf. Plast. Compos.* **2019**, *38*, 835–845. [CrossRef]
109. Blythe, A.; Fox, B.; Nikzad, M.; Eisenbart, B.; Chai, B.X.; Blanchard, P.; Dahl, J. Evaluation of the failure mechanism in polyamide nanofibre veil toughened hybrid carbon/glass fibre composites. *Materials* **2022**, *15*, 8877. [CrossRef]
110. Blythe, A.; Fox, B.; Nikzad, M.; Eisenbart, B.; Chai, B.X. Stiffness Degradation under Cyclic Loading Using Three-Point Bending of Hybridised Carbon/Glass Fibres with a Polyamide 6, 6 Nanofibre Interlayer. *J. Compos. Sci.* **2022**, *6*, 270. [CrossRef]
111. Beckermann, G.W. Nanofiber interleaving veils for improving the performance of composite laminates. *Reinf. Plast.* **2017**, *61*, 289–293. [CrossRef]
112. Mohammadi, R.; Najafabadi, M.A.; Saghafi, H.; Saeedifar, M.; Zarouchas, D. A quantitative assessment of the damage mechanisms of CFRP laminates interleaved by PA66 electrospun nanofibers using acoustic emission. *Compos. Struct.* **2021**, *258*, 113395. [CrossRef]

Disclaimer/Publisher's Note: The statements, opinions and data contained in all publications are solely those of the individual author(s) and contributor(s) and not of MDPI and/or the editor(s). MDPI and/or the editor(s) disclaim responsibility for any injury to people or property resulting from any ideas, methods, instructions or products referred to in the content.